Mon. Not. R. Astron. Soc. **000**, 1–9 (0000) Printed 1 February 2008 (MN LATEX style file v1.4)

Magnetic ionization fronts II: Jump conditions for oblique magnetization

R.J.R. Williams[1,2], J.E. Dyson[2] and T.W. Hartquist[2]
[1] *Department of Physics and Astronomy, Cardiff University, PO Box 913, Cardiff CF24 3YB*
[2] *Department of Physics and Astronomy, The University, Leeds LS2 9JT*

arXiv:astro-ph/0001116v1 7 Jan 2000

Received **INSERT**; in original form **INSERT**

ABSTRACT
We present the jump conditions for ionization fronts with oblique magnetic fields. The standard nomenclature of R- and D-type fronts can still be applied, but in the case of oblique magnetization there are fronts of each type about each of the fast- and slow-mode speeds. As an ionization front slows, it will drive first a fast- and then a slow-mode shock into the surrounding medium. Even for rather weak upstream magnetic fields, the effect of magnetization on ionization front evolution can be important.

Key words: MHD – H II regions – ISM: kinematics and dynamics – ISM: magnetic fields.

1 INTRODUCTION

The sequence of evolution of the H II region around a star with a strong ionising radiation field which turns on rapidly is well known (Kahn 1954; Goldsworthy 1961; see also Spitzer 1978, Osterbrock 1989 or Dyson & Williams 1997). Initially, the ionization front (IF) between ionized and neutral gas moves outwards at a speed limited by the supply of ionizing photons, but it begins to decelerate as the ionizing flux at the front surface is cut by geometrical divergence and absorption by recombined atoms within the front. Eventually, when the speed of the front decreases to roughly twice the sound speed in the (now highly overpressured) ionized gas, a shock is driven forwards into the neutral gas ahead of the front. Before this stage, the front is referred to as R-type, while subsequently it is referred to as D-type. The shock propagates outwards, gradually weakening, until, in principle, the H II region eventually reaches pressure equilibrium with its surroundings.

Where the external medium has an ordered magnetic field, the obvious critical flow speeds are the fast, Alfvén and slow speeds rather than the isothermal sound speed. Redman et al. (1998, hereafter Paper I) studied IFs with the magnetic field vector in the plane of the front, and found that the fast-mode speed plays the same role as the sound speed does in the hydrodynamic case. In this paper, we extend their work to treat the case of an IF moving into a medium in which the magnetic field is oblique to the direction of propagation of the front (note also we here follow the more conventional usage in which the magnetic fields are termed parallel or perpendicular with respect to the front-normal).

Jump conditions for IFs with oblique magnetization have previously been studied by Lasker (1966). Here we consider a wider range of upstream magnetic fields, since observations have shown that higher magnetic fields are found around H II regions than once thought likely (e.g. Roberts et al. 1993; Roberts et al. 1995). We determine the properties of the jumps as functions of upstream conditions, using the velocity of the front as a parameter rather than as the variable for which we solve. We use evolutionary conditions to isolate the stable IF solutions, and verify these conclusions for a simple model of the internal structure of the fronts and using numerical simulations. We find that rather weak parallel magnetic fields can lead to a substantial decrease in the D-critical (i.e. photoevaporation) velocity from dense clumps except where the magnetic field is exactly parallel to the IF, and also find additional solutions to the jump conditions in the range of front velocities forbidden by the hydrodynamical jump conditions, which were not considered by Lasker.

In the following sections, we present the jump conditions for MHD shocks (Section 2), and discuss the regions for which evolutionary conditions suggest that these solutions are stable (Section 3). We verify that the evolutionary solutions are those with resolved internal structures for one simple model for the internal structure of the fronts (Section 4). In the context of these results, we discuss the development of an IF over time (Section 5) and illustrate this development using numerical models (Section 6).

Finally (in Section 7), we summarize our results, and provide an example of their application to observations of the H II region S106. Our physical interpretation of the development of MHD IFs will, we hope, facilitate the future application of these results.

© 0000 RAS

2 JUMP CONDITIONS

We orient axes so that $\hat{\boldsymbol{z}}$ is normal to the front, and (without loss of generality) that the upstream velocity and magnetic field are in the (x, z) plane. We use the usual MHD jump conditions:

$$[\rho v_z] = 0 \quad (1)$$
$$[\rho v_z^2 + p + B_x^2/8\pi] = 0 \quad (2)$$
$$[\rho v_z v_x - B_z B_x/4\pi] = 0 \quad (3)$$
$$[B_z] = 0 \quad (4)$$
$$[v_x B_z - v_z B_x] = 0, \quad (5)$$

except that instead of using the energy flux condition, we adopt the isothermal equation of state $p = \rho c_{\rm s}^2$ where the sound speed, $c_{\rm s}$, increases across the front but is constant on either side of it. We use subscripts 1 and 2 to denote upstream and downstream parameters, respectively, and write $v_x = u_{1,2}$, $v_z = v_{1,2}$, $c_{\rm s} = c_{1,2}$ and $B_x = B_{1,2}$. Hence

$$\rho_1/\rho_2 = v_2/v_1 \equiv \delta \quad (6)$$
$$\rho_2(v_2^2 + c_2^2) + B_2^2/8\pi = \rho_1(v_1^2 + c_1^2) + B_1^2/8\pi \quad (7)$$
$$\rho_2 v_2 u_2 - B_z B_2/4\pi = \rho_1 v_1 u_1 - B_z B_1/4\pi \quad (8)$$
$$u_2 B_z - v_2 B_2 = u_1 B_z - v_1 B_1 \quad (9)$$

Equations (6), (8) and (9) give

$$B_2 = \frac{m_1^2 - 2\eta_1}{\delta m_1^2 - 2\eta_1} B_1, \quad (10)$$

where $m = v/c_{\rm s}$ and we define $\eta = B_z^2/8\pi\rho c^2$ and $\xi = B_x^2/8\pi\rho c^2$ (the z and x contributions to the reciprocal of the plasma beta). The dependence on the upstream transverse velocity has disappeared, as expected as a result of frame-invariance.

In equation (7), we substitute with (10) for B_2 and use equation (6) to eliminate ρ_2 and v_2 to find that, so long as $\delta \neq 0$ and $\delta m_1^2 \neq 2\eta_1$, the dilution factor δ is given by the quartic equation (see also Lasker 1966)

$$\begin{aligned} & m_1^6\delta^4 - m_1^4(1 + m_1^2 + 4\eta_1 + \xi_1)\delta^3 \\ & + m_1^2(\alpha m_1^2 + 4\eta_1(1 + m_1^2 + \eta_1 + \xi_1))\delta^2 \\ & + (\xi_1 m_1^4 - 4\eta_1(\eta_1 + m_1^2(\eta_1 + \xi_1 + \alpha)))\delta \\ & + 4\alpha\eta_1^2 = 0, \end{aligned} \quad (11)$$

where $\alpha = (c_2/c_1)^2$ (100 is a typical value). It is easily verified that this equation has the correct form in the obvious limiting cases (of isothermal MHD shocks where $\alpha = 1$, and perpendicular-magnetized IFs where $\eta_1 = 0$, see Paper I).

3 SOLUTIONS

Equation (11) relates the dilution factor, δ, to the upstream properties of the flow. Its roots can be found by standard techniques. If the flow is to have a unique solution based only on initial and boundary conditions, then some of these roots must be excluded. It is possible to exclude roots on the basis that they correspond to flows that do not satisfy an evolutionary condition, analogous to that long used in the study of MHD shocks. The evolutionary condition is based on the requirement that the number of unknowns in the jump conditions matches the number of constraints applied to the flow (e.g. Jeffrey & Taniuti 1964). For MHD shocks, the number of characteristics entering the shock must be two greater than the number leaving it (since the number of independent shock equations is equal to the number of conserved variables and if there are no internal constraints on the front structure).

The applicability of the evolutionary conditions to MHD shocks has been the subject of controversy in the recent past (e.g. Brio & Wu 1988; Kennel, Blandford & Wu 1990), with various authors suggesting that intermediate shocks (i.e. shocks which take the flow from super- to sub-Alfvén speeds) may be stable. However, Falle & Komissarov (1997; 1999) have shown that the non-evolutionary solutions are only stable when the symmetry is artificially constrained, so that the magnetic fields ahead of and behind the shocks are precisely coplanar. In any cases in which the boundary conditions differed from this special symmetry, the solutions including non-evolutionary shocks were found to be unstable.

The equations governing the dynamics across an IF are no longer a system of hyperbolic conservation laws, since the ionization source term cannot be neglected on the scale of the front. It seems reasonable to apply analogous evolutionary and uniqueness conditions, but the mathematical proofs for hyperbolic conservation laws with dissipation (Falle & Komissarov 1999) no longer apply. The 'strong' evolutionary conditions suggest that for IF the number of incoming characteristics is equal to the number of outgoing characteristics, since applying the ionization equation means that there is an additional constraint on the velocity of the front.

Solutions which are under-specified by the external characteristic constraints, termed 'weakly evolutionary', may occur if there are internal constraints, as is the case for strong D-type IFs in hydrodynamics. Stable weakly evolutionary solutions only occur for limited classes of upstream parameters which depend on the internal structure of the fronts. Where the number of characteristics entering the front is greater than suggested by the evolutionary conditions, the solution can be realized as an MHD shock leading or trailing an evolutionary IF.

In the limit in which α tends to unity from above, the phase change through the IF has no dynamical consequences, and the IF jump conditions approach those for isothermal MHD shocks. This can be seen if we rewrite equation (11) as

$$\begin{aligned} & (\delta - 1)[m^6\delta^3 - m^4(1 + 4\eta + \xi)\delta^2 \\ & + m^2(4\eta(1 + \eta + \xi) - m^2\xi)\delta - 4\eta^2] \\ & = -(\alpha - 1)[m^2\delta - 2\eta]^2. \end{aligned} \quad (12)$$

The IF solution which satisfies the strong evolutionary conditions becomes the trivial ($\delta = 1$) solution of the MHD jump condition. The other solutions to the IF jump conditions become non-evolutionary or evolutionary isothermal MHD shocks. The analysis of Falle & Komissarov (1999) rules out the former as physical solutions. The latter are treatable as separate discontinuities, which will propagate away from the IF when the flow is perturbed, since the coincidence between the speeds of the shock and of the IF will be broken. This argument by continuity supports the use of the evolutionary conditions for IFs.

As a result of this discussion, we will proceed for the present to isolate solutions in which the number of charac-

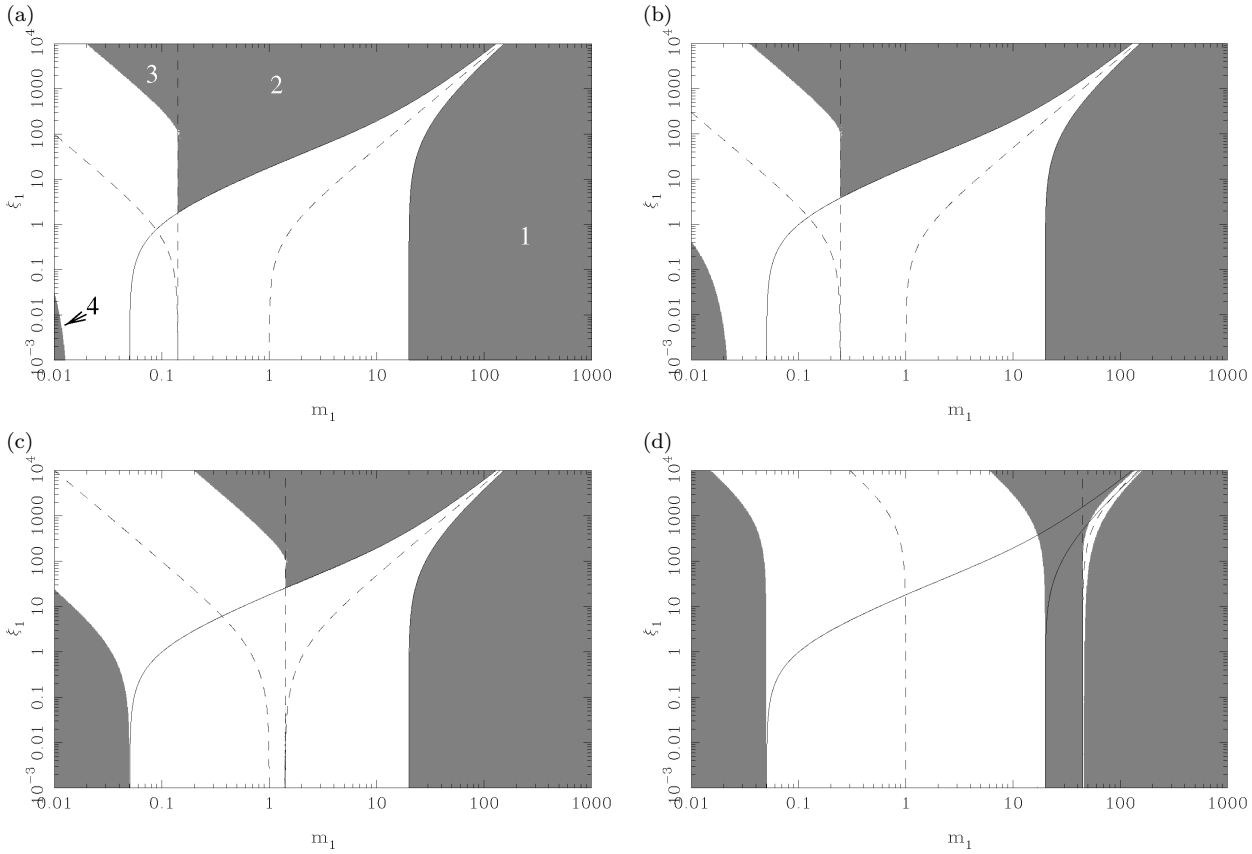

Figure 1. Allowed obliquely magnetized IFs (shown grey). The solid lines show the edges of the forbidden region for $\eta = 0$, and the dashed lines where the inflowing gas moves at the slow, Alfvén and fast speeds, from left to right. The grey regions correspond to allowed weak solutions for (a) $\eta_1 = 0.01$, (b) $\eta_1 = 3{\times}10^{-2}$, (c) $\eta_1 = 1$, and (d) $\eta_1 = 1000$. In (a) the regions are labelled: 1 – the $1 \rightarrow 1$, fast-R solutions; 2 – the $2 \rightarrow 2$, fast-D solutions; 3 – the $3 \rightarrow 3$, slow-R solutions; 4 – the $4 \rightarrow 4$, slow-D solutions. The fast-D and slow-R regions are separated by the dashed line at the upstream Alfvén speed. Critical solutions will be expected at the right-most edge of the slow-D type region (a $4 \rightarrow 3$ IF) and of the fast-D type region (a $2 \rightarrow 1$ IF).

teristics entering an IF is equal to the number leaving it (and discuss in Section 4 the weakly evolutionary solutions for a simplified model of the internal structure of IFs). The velocity of fronts obeying the strong evolutionary conditions must be between the same critical speeds in the upstream and downstream gas (somewhat confusingly, the fronts which obey the strong evolutionary conditions are termed 'weak' in the standard nomenclature of detonations and IFs). We follow the usual classification of flow speeds relative to the fast, Alfvén and slow mode speeds $1 > v_{\rm f} > 2 > v_{\rm a} > 3 > v_{\rm s} > 4$, so the allowed fronts are $1 \rightarrow 1$, $2 \rightarrow 2$, $3 \rightarrow 3$ and $4 \rightarrow 4$. By analogy with the nomenclature of non-magnetized IF, we call these fast-R, fast-D, slow-R and slow-D type IF, respectively.

The panels of Fig. 1 show regions of m_1 and ξ_1 space corresponding to evolutionary MHD IFs for several values of η_1. In the figures, we see regions corresponding to the two distinct classes of R- and D-type solutions. The flows into the R-type fronts are super-fast or super-slow, while those into the D-type fronts are sub-fast or sub-slow. At the edges of the regions of solutions either the velocity into the front is the Alfvén speed or the exit velocity from the front is equal to a characteristic speed (i.e. the fast mode speed at the edge of the fast-R region, etc.). For comparison, the solid lines on these plots show the edges of the forbidden region for perpendicular magnetization ($\eta_1 = 0$, see Paper I): these lines reach $\xi_1 = 0$ at the edges of the forbidden region for unmagnetized IF, $0.05 \lesssim m_1 \lesssim 20$.

Since equation (11) is a cubic in m_1^2, quadratic in η_1 and linear in α and ξ_1, there is no simple analytic form for the boundaries of the regions. However, certain critical values can be determined analytically. For $\eta_1 \lesssim 2\alpha$, the slow-R-critical line terminates where it hits the Alfvén speed at $\xi_1 = \alpha - 1$, while the position at which the fast D-critical line terminates is given by

$$(1 + 2\eta_1 + \xi_1)^2 = 8\alpha\eta_1. \tag{13}$$

These points are linked, respectively, by steady switch-off and switch-on shocks to the points on the limiting slow-D and fast-R critical loci at which these loci hit the axis $\xi_1 = 0$. The intercept between the slow-D critical locus and the axis is at

$$m_1^2 = 2\eta_1 \frac{1 - 2\eta_1}{\alpha - 2\eta_1}, \tag{14}$$

for $2\eta_1 \leq (\alpha - \sqrt{\alpha^2 - \alpha})$, beyond which the limiting value is $m_1^2 \simeq 1/(4\alpha)$ as for D-critical hydrodynamic IF. To il-

lustrate the reason for this change in solution, we rewrite equation (11) for $\xi_1 = 0$ as

$$(m_1^2\delta - 2\eta)^2(m_1^2\delta^2 - (1+m_1^2)\delta + \alpha) = 0. \quad (15)$$

The flow leaving a front with no upstream perpendicular component of magnetic field can be either at the Alfvén speed or at the velocity of the corresponding non-magnetized IF. Where the flow is in the region beyond the edge of the slow-D-critical region shown in Figure 1 (a) or (b), the root of equation (15) for flow out at the Alfvén speed is not a real solution, since satisfying equation (7) would require that $B_2^2 < 0$.

Even for as small a ratio between magnetic and thermal energy upstream of the front as implied by $\eta_1 = 0.01$, the effect of parallel magnetization on the slow-D-critical velocity is dramatic. Only once $\eta_1 \lesssim 1/(8\alpha)$ (so the Alfvén speed in the upstream gas is below the unmagnetized D-critical speed) does the fast-critical locus reach $\xi_1 = 0$, so that the parallel magnetization may be ignored. As η_1 increases, the vertical line at the Alfvén speed moves across the plot (see Figure 1), decreasing the region of fast-mode IFs and increasing that of slow-mode IFs. When $\eta_1 \to \infty$ (a very strong parallel magnetic field), the (slow-mode) forbidden region is identical to that in the unmagnetized case (independent of ξ_1).

If the upstream flow is at the Alfvén velocity, $m_1^2 = 2\eta_1$, then the physical solution (when due care is taken with the singularity of equation (10)) is often at $\delta = 1$, i.e. the ionization of the gas does not change the flow density and it remains at the Alfvén speed. Both classes of D-type front have $\delta > 1$ (rarefy the gas), while both classes of R-type have $\delta < 1$ (compress it). The perpendicular component of the magnetic field, B_x, increases in a fast-R- or slow-D-type IF, while it decreases in a fast-D- or slow-R-type.

We will now study the internal structure of the fronts for one simple model.

4 RESOLVED FRONTS

Up to now we have assumed, by investigating the jump conditions, that the processes within the IF take place on scales far smaller than those of interest for the global flow problem. In fact, the flow structure within an ionization front will vary smoothly on scales comparable to the ionization distance in the neutral gas. The flow may take several recombination lengths behind the front to relax to equilibrium. Here we describe the internal structure of MHD IF in one simple approximation, that the temperature of the gas varies smoothly through the front but the flow obeys the inviscid MHD equations throughout (as used in the study of hydrodynamic IF structure by Axford 1961). We shall see that, in this approximation, only fronts obeying the evolutionary conditions can have smooth structures. For the structures to be generic, the jumps across them must satisfy the strong evolutionary conditions, although singular classes of weakly evolutionary fronts with internal constraints on their flow structures are also possible.

In this model the form of an IF is given by the variation of the roots of equation (12) with the temperature of the gas, specified by α. The left hand side of this equation is a quartic independent of α, which is positive at $\delta = 0, \infty$ and zero at

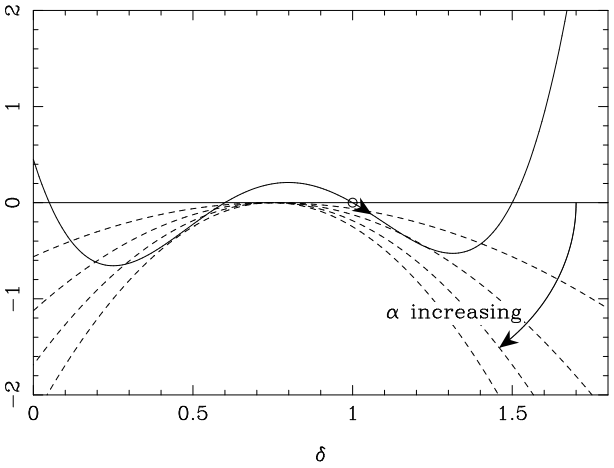

Figure 2. Schematic plot of equation (12), where the solid curve corresponds to the l.h.s. while the dashed curves correspond to the r.h.s. for various values of α. The points where the solid curve passes through zero give the solutions of the isothermal shock jump conditions.

$\delta = 1$, and has two or four positive roots (since the condition that its value is zero is the normal MHD shock condition for isothermal gas, cf. Anderson 1963). The right hand side is a quadratic, which is zero at $m_1^2\delta = 2\eta$ and depends on α through its (negative) scale. If the value of α increases steadily through the front, the manner in which the solutions vary can be followed, as illustrated by the schematic plot, Fig. 2.

For the upstream conditions ($\alpha = 1$), there will be either two or four solutions where the quartic curve crosses the axis. Of these, one is the trivial solution, $\delta = 1$, and at most one corresponds to an evolutionary shock.

When internal heating occurs in an IF, the solutions at a given α correspond to where the solid curve in Fig. 2 crosses the corresponding dashed curve, $-(\alpha - 1)(m_1^2\delta - 2\eta_1)$. If gas enters the IF at the point marked $\circ$, in region 2 between the Alfvén speed and the fast mode speed, then it can move following the arrow as α increases. For sufficiently large α, the dashed curve becomes tangent to the solid curve: when this occurs, the gas is moving at the slow- or fast-mode speed, and the IF is called a critical front. In between the initial and final solutions, smooth, steady IF solutions must remain between the same characteristic speeds as they were when they started. The strong evolutionary conditions give just those cases in which a front structure calculated for a smoothly varying, monotonically increasing α (and non-zero perpendicular magnetic field) has a continuous solution from the upstream to the downstream case.

When the upstream flow is at the fast or the slow critical speed, the l.h.s. of equation (12) has a second root $\delta = 1$. Thus for $\alpha > 1$, this pair of roots disappears, and a forbidden region is generated. For $\alpha \leq 1$ there is no forbidden region.

For any α, the points where the solid curve crosses the dashed curve in Fig. 2 are related to each other by the isothermal MHD shock jump conditions, so a steady shock can form anywhere within the IF structure for identical upstream and downstream conditions. However, since such a flow is over-specified, the equality of the speed between the shock and IF is a coincidence which will be broken by any

perturbation of the flow (in which case the shock will escape from one or other side of the IF). This situation is in direct analogy with strong R-type IFs in unmagnetized flows.

Strong D-type fronts, for which the exhaust leaves the front rather above the critical speed, can occur where the heating is not monotonic. For these, the highest temperature is attained when the flow is at the critical speed (i.e. the curves in Figure 2 become tangent exactly at the highest value of α), and as it subsequently cools the solution can move back up the other branch. These fronts will form a more restrictive limiting envelope on the allowed weak solutions than that given by the critical solutions. The evolutionary conditions are necessary but not sufficient, so this behaviour would be expected when more detailed physics was included. The actual envelope will correspond to the case for critical fronts with exhausts at the highest temperature attained within the front. Since unmagnetized IF models suggest that any overshoot in the temperature of the gas is likely to be small, the envelope will probably not differ greatly from that found for critical solutions, although the transonic nature of these fronts can be important in determining the structure of global flows.

Equation (10) suggests that no MHD flow can pass through the Alfvén velocity (where $\delta m_1^2 = 2\eta_1$) in a front unless it has zero perpendicular magnetic field. Heating the gas will generally move the flow in regions 2 and 3 away from the Alfvén speed in any case (see Figures 2 and 3). However, where the perpendicular magnetic field *is* zero, a smooth, weakly evolutionary, front structure can be found (the internal constraint being zero perpendicular magnetic field). The internal structure will be identical to an unmagnetized IF. Indeed, the strong-D hydrodynamic front can become, by analogy, an 'extra-strong' front which passes through both the Alfvén and sound speeds (for zero perpendicular field, the slow and fast velocities are each equal to one of these).

By analogy with equation (10), the y-components of velocity and magnetic field are zero everywhere if the MHD equations apply throughout the front (except if it were to pass through the Alfvén velocity). Components in these directions *can* be generated if the velocity coupling between different components of the fluid – electrons, ions, neutrals or dust – is not perfect (as in shock structures, Pilipp & Hartquist 1994; Wardle 1998). These components must, however, damp at large enough scales: far beyond the front the magnetic field must be in the same plane and of the same sign as the upstream field, from the evolutionary conditions. Exactly this behaviour has been found to occur in time-dependent multifluid models of MHD shocks (Falle, private communication). A full treatment of ionization fronts in multicomponent material is, however, beyond the scope of the present paper.

5 TIME DEVELOPMENT

In this section, we discuss the development of the IF in a magnetized H II region, by combining the well-understood development of IF in unmagnetized environments with the classes of physical roots of equation (11) found above.

An IF driven into finite density gas from a source which turns on instantaneously will start at a velocity greater than the fast-R-critical velocity. Unless the density decreases rapidly away from the source, the speed of the front decreases so that eventually the ionized gas exhaust is at the fast-mode speed (at the fast-R-critical velocity). When this occurs, two roots of equation (11) merge, and become complex for smaller m_1. As a result, the front will then have to undergo a transition of some sort. As in the unmagnetized case (Kahn 1954), if the size of the ionized region is large compared to the lengthscales which characterise the internal structures of shocks and IFs, the IF will evolve through emitting (one or more) shocks. The evolution of an initial IF discontinuity can be treated as a modified Riemann problem because the speed of the IF is determined by the flow properties on either side of it, together with the incident ionizing flux which we assume varies slowly. The development of this modified Riemann problem will be self-similar, just as for conventional Riemann problems. One complication is that the IF may be located within a rarefaction wave, but this does not occur for the circumstances we discuss in the present section.

The simplest possibility for a slowing fast-R-critical IF is that it will become fast-D-type by emitting a single fast-mode shock. This has obvious limits to the cases where the magnetization is zero (where the shock is a normal hydrodynamic shock), and where it is purely perpendicular. If the speed of the IF is specified by the mass flux through it, then the leading shock driven into the surrounding neutral gas must be a fast-mode shock, since the upstream neutral gas must still be advected into the combined structure at more than the Alfvén speed after the transition, and so only a fast-mode shock can escape.

While there may be no fast-D-type solutions at the value of ξ_1 which applied for the fast-R-type front, the fast-mode shock moving ahead will act to increase the value of ξ upstream of the IF, since the (squared) increase in the perpendicular component of the magnetic field dominates over the increase in the gas density after the shock. At fast-R-criticality, there is in general a second solution with the same upstream and downstream states in which a fast-mode shock leads a fast-D-critical IF, because the l.h.s. of equation (12) (for which a zero value implies an isothermal shock solution) is positive for large δ and for post shock flow at the Alfvén speed (i.e. $m_1^2\delta = 2\eta_1$), unless the flow into the front is at the Alfvén velocity, or η_1 or ξ_1 is zero. For example, for a downstream state $\eta_2 = \xi_2 = 5{\times}10^{-3}$, there are two evolutionary solutions: a $1 \rightarrow 1$ front with $\eta_1 = 0.994$, $\xi_1 = 0.248$, $m_1 = 20.0$ and $\delta = 0.503$, and a $2 \rightarrow 2$ front with $\eta_1 = 3.11{\times}10^{-2}$, $\xi_1 = 11.1$, $m_1 = 0.625$ and $\delta = 16.1$. Figure 1 parts (c) and (b), respectively, contain points which correspond to these solutions. These two upstream states are linked by a fast-mode shock with the same velocity as the IF. Thus the emission of a single fast-mode shock is a valid solution of the modified Riemann problem which occurs as the flow passes through criticality *whatever* the internal structure of the shock and IF, so long as the evolutionary shocks and IFs exist. (Since the l.h.s. of equation (12) is greater than zero so long as $\eta_1 \neq 0$ for $\delta = 0$, an equivalent argument holds for slow-critical transitions.)

It is possible that further waves may be emitted at the transition, for instance a slow-mode shock into the neutral gas together with a slow-mode rarefaction into the ionized gas. For the model resolved IF, this seems unlikely to occur unless the flow velocity reaches the slow-mode speed some-

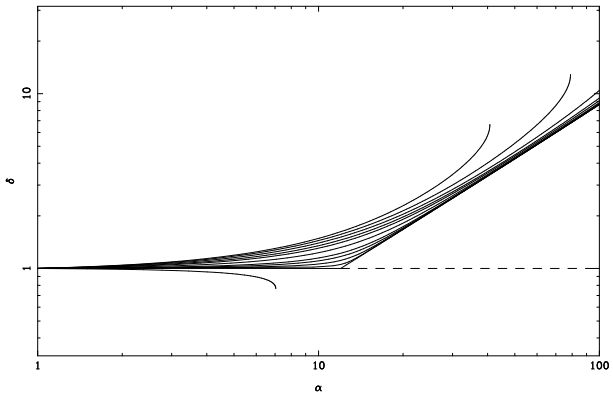

Figure 3. Plot of the dilution factor, δ, within magnetized IFs for $\eta_1 = 3{\times}10^{-2}$ and $\xi_1 = 11$ (cf. Figure 1(b) and the numerical example in the text), and m_1^2 decreasing towards $2\eta_1$ (with values for m_1, plotted from top to bottom of the fan entering at $\delta = 1$, of $m_1 = 1$, 0.7, 0.5, 0.4, 0.35, 0.3, 0.27, 0.26, 0.252, 0.247, the critical solution and 0.22). Also shown dashed are the non-evolutionary Alfvén solution for critical m_1. The solutions terminate for $\alpha < 100$ for both high and low values of m_1. Note also the development of the gradient discontinuity at $\alpha = \xi_1 + 1$ in the density structure.

where within the fast-D-critical IF. These other solutions are not seen in our numerical simulations below. Additional solutions would also make the development of the IF non-unique, if the simpler possibility is allowed.

The fast-critical transition may be followed using the jump conditions for a front with its exhaust at the fast-mode speed (i.e. a fast-critical front). In the smoothly-varying α model of Section 4, the upstream and downstream states can be joined by a front in which an isothermal MHD shock is at rest in the IF frame *anywhere* within the IF structure, since the quantities conserved through the front are also conserved by the shock. The evolution of an IF through criticality will occur by an infinitesimally-weak fast-mode wave at the exhaust of the IF moving forward through its structure and strengthening until it eventually escapes into the neutral gas as an independent shock (as illustrated for recombination fronts by Williams & Dyson 1996).

The escaping fast-mode shock leads to a near-perpendicular field configuration upstream of the IF. This boost in the perpendicular component is required if the transition is to proceed though the fast-D type solutions, which, as Figure 1 illustrates, are near-perpendicular (large ξ_1) except where B_z is very large or very small. This will result in a rapid change in downstream parameters across a front where the upstream field is nearly parallel to the IF. As an example, the flow downstream of the IF will either converge onto or diverge from lines where the upstream magnetic field is parallel to the ionization front, and as a result may produce inhomogeneities in the structure of H II regions on various scales (from bipolarity to clumps).

As the velocity of the front decreases further, eventually it will approach the Alfvén speed. We find that the evolution depends qualitatively on whether $\alpha - 1$ is smaller than ξ_1. In Fig. 3, we plot δ as a function of α for a range of values of m_1 (i.e. the internal structure of the fronts in the simple model of Section 4). We take $\eta_1 = 3{\times}10^{-2}$ and $\xi_1 = 11$, corresponding to our numerical example above, so the ratio of the upstream Alfvén speed to the upstream isothermal sound speed is 0.245. For m_1 slightly larger than 0.245 (i.e. just super-Alfvén), the curves remain flat until α is close to $\xi_1 + 1$ and then turn upwards when they reach this value. If the value of α in the fully ionized gas were less than $\xi_1 + 1$, the solutions would move through a case where the flow is of uniform density and moves at the Alfvén speed throughout the front before becoming slow-R-critical for some $m_1^2 < 2\eta$, as can be seen in the leftmost part of Fig. 3, for fronts in which the maximum α is smaller than 12.

For larger values of α, however, the solutions develop a gradient discontinuity in their structure when the inflow is at the Alfvén speed, $m_1^2 = 2\eta$. At this discontinuity, the transverse component of the magnetic field becomes zero (i.e. switch-off occurs). Once the propagation speed of the IF drops below the Alfvén speed, there is no form of steady evolutionary structure with a single wave in addition to the IF which is continuous with that which applied before. Non-evolutionary $3 \rightarrow 2$ type solutions do exist for fronts just below this limit, but in numerical simulations (see Section 6) these break up. A slow-mode switch-off shock moves into the neutral gas and a slow-mode switch-on rarefaction is advected away into the ionized gas. Between them, these waves remove the parallel component of magnetic field at the D-type IF between them. A precursor for the rarefaction is apparent in internal structure of the critical front, Figure 3. We find in numerical simulations that the IF which remains is trans-Alfvénic. Note that a steady resolved structure is possible for such (weakly evolutionary) fronts only because it has exactly zero parallel field throughout.

Analogous processes must occur in an accelerating *fast*-mode IF with weak parallel magnetization when η_1 is very large: in Fig. 1 (d), it is the fast-D-critical line rather than the slow-R-critical line which meets the Alfvén locus at finite ξ_1.

6 NUMERICAL SOLUTIONS

In this section, we present some numerical examples to illustrate the processes discussed in the preceding sections. We have implemented linear scheme A as described by Falle, Komissarov & Joarder (1998) in one dimension, and added an extra conserved variable corresponding to the flow ionization. To study the local development of the IFs we have neglected recombination terms and just chosen to set the mass flux through the ionization flux as a function of time.

Figure 4(a) shows the propagation of an IF into gas with density 1, $B_z = 0.3\sqrt{4\pi}$, $B_x = 2\sqrt{4\pi}$. We reset the flow temperature at the end of each time step so that $p = (0.1 + 0.9x)\rho$ (the temperature ratio between ionized and neutral gas is rather small so that any shells of shocked neutral gas are more easily resolved). For these values, the characteristic speeds in the neutral gas are $v_{\rm s} = 0.046$, $v_{\rm a} = 0.3$ and $v_{\rm f} = 2$. In the first figure, the incident flux varies as $80/(20+t)$, and the transitions through fast-R, fast-D and slow-D are clearly visible, while the slow-R stage (which is often narrow in the parameter space of Fig. 1) is less clear.

In Figure 4(b) the upstream conditions are the same, but the flux was set to a constant value of 0.26 in order to isolate the slow-R transition. This is between the upstream slow-mode and Alfvén speeds, and equation (11) predicts that a slow-R transition exists which will increase the flow

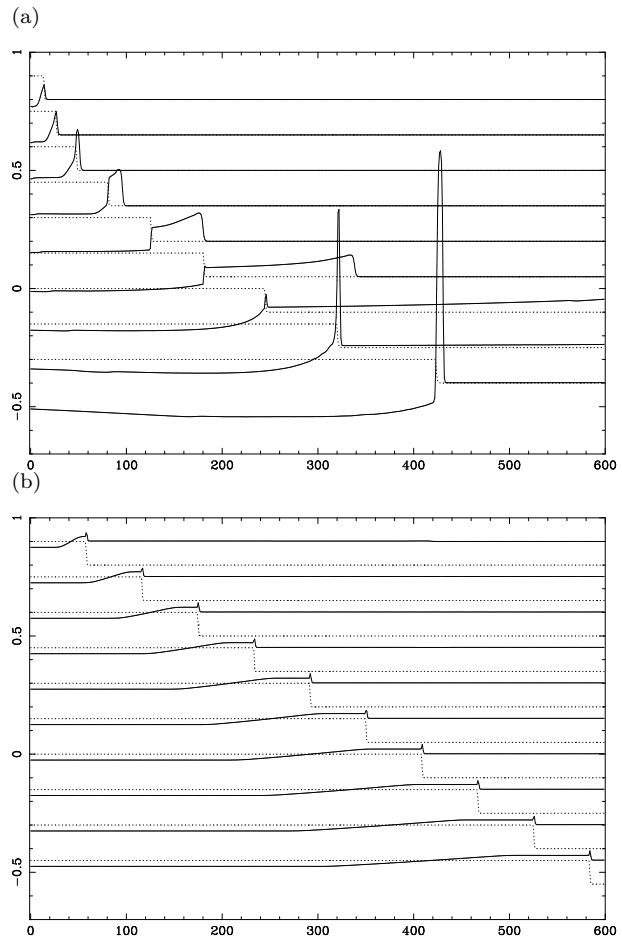

Figure 4. Evolution of an oblique magnetized IF for (a) gradually decreasing incident radiation intensity; (b) constant intensity chosen to show slow-R-type IF. In (a), the frames show log base 10 of density (solid) and ionization fraction (dotted), offset by a constant between each plot, plotted at times $4, 8, 16, ..., 1024$. The topmost plot shows a fast-R IF, while third, fourth and fifth show a fast-D IF together with a fast shock moving to the right. In the next two, the IF changes to a slow-R type while in the final two a slow shock has moved off leaving a slow-D type behind. In (b), a more clearly resolved slow-R type front is shown. In this figure, the density is plotted linearly, scaled by a factor 0.1, and the plots are at times $200, 400, ..., 2000$.

density from 1 to 1.18 (for comparison, the $3 \rightarrow 4$ jump relations require the density to increase to 1.75). In the simulation, a weak fast-mode wave propagates off from the IF initially, but does not greatly change the upstream conditions. The slow-R IF which follows it increases the density, and is backed by a rarefaction because of the reflective boundary condition applied at the left of the grid. The small overshoot within the front is presumably due to numerical viscosity, and can be removed by broadening the IF (e.g. by the method described in Williams 1999). The plateau between the rarefaction and the IF has density 1.22, which is in adequate agreement with the jump conditions (particularly when account is taken of the slight perturbation of the conditions upstream of the front).

These numerical solutions illustrate the orderly progression of a magnetized IF through the various transitions described in the previous section. In a realistic model, however, the density perturbations generated by the transitions will have important effects on the evolution, as the consequent changes in recombination rates alter the flux incident on the IF. These processes should ideally be studied in the context of a two- or three-dimensional global model for the evolution of magnetized H II regions, which is beyond the scope of the present paper.

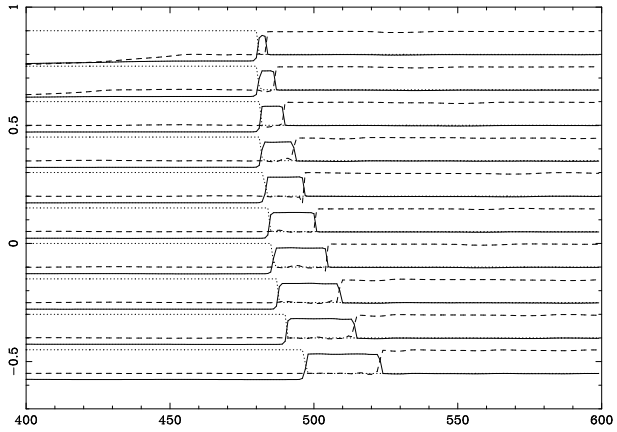

Figure 5. Evolution of an IF from an initially non-evolutionary solution. The curves show the density (0.1 times the log base 10, solid), ionization fraction (multiplied by 0.1, dotted) and $0.1 \times B_x/\sqrt{4\pi}$ (dashed), plotted at times $400, 800, 1200, ..., 4000$ with an offset between each plot.

In Figure 5, we illustrate the development of the flow from initial conditions in which a non-evolutionary IF is stationary in the grid. The upstream (neutral) gas has density 1, $B_z = 0.3\sqrt{4\pi}$, and $B_x = \sqrt{4\pi}$ and moves into the front at $v_z = -0.253$ (with no transverse velocity), while the downstream (fully ionized) gas has $\rho = 0.423$, $v_z = -0.598$, $v_x = 1.688$ $B_z = 0.3\sqrt{4\pi}$, and $B_x = -0.424\sqrt{4\pi}$ so the IF is of $3 \rightarrow 2$ type. We set the pressure as above, and the value of the incident flux as 0.253 so the initial IF would remain steady in the grid. The IF breaks up immediately, driving a slow-mode shock away to the right, into the neutral gas, while a slow-mode rarefaction moves away to the left, into the ionized gas. The D-type IF which remains is marginally trans-Alfvénic, but has zero transverse magnetic field.

To study this further, in Fig. 6, we illustrate a simulation of an IF close to the (hydrodynamic) D-critical condition, with a parallel magnetic field which makes it trans-Alfvénic. When perturbed with small but significant perpendicular field components, this IF again switches off these fields by emitting slow-mode waves. It remains stable, satisfying the hydrodynamic jump conditions as a weakly evolutionary solution of the MHD jump conditions.

7 CONCLUSIONS

We have presented the jump conditions for obliquely-magnetized ionization fronts. We have determined the regions of parameter space in which physical IF solutions occur, and have discussed the nature of the interconversions between the types of front. Fast-D and slow-R solutions with high transverse fields are found in the region of front veloci-

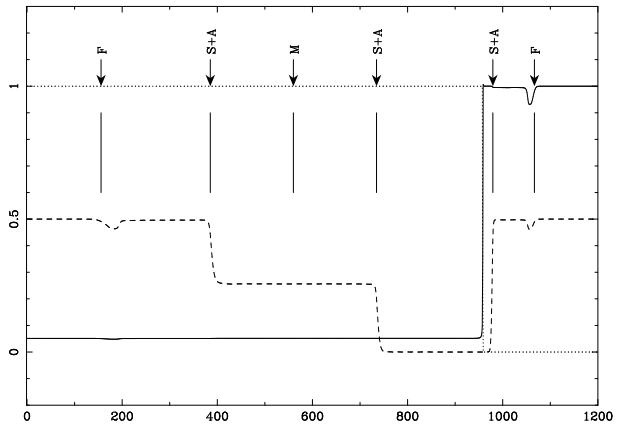

Figure 6. Evolution of an IF obeying the hydrodynamic D-critical conditions at rest, perturbed by an initial magnetic field. The upstream density is 1 and velocity is -0.0513, while the downstream density is 0.0513 and velocity is -1. A parallel field of $B_z = 0.1\sqrt{4\pi}$ means this front is trans-Alfvénic. The IF is perturbed with a perpendicular magnetic field of magnitude $0.03\sqrt{4\pi}$, in different planes up- and down-stream. The solid line shows the density, the dotted line is the ionization fraction and the dashed line is one component of the perpendicular magnetic field (which has been scaled to a maximum amplitude of 0.5). Also shown are the positions of the characteristic waves from the initial discontinuity (F is fast, A is Alfvén, S is slow, M is mass), based on the initial states. The waves which change the magnetic field are, from left to right, a slow-mode shock plus an Alfvén wave, a slow-mode switch-on rarefaction (which switches *off* the field as it is being advected away from the IF) and a slow-mode switch-off shock propagating into the upstream gas. The front which remains is trans-Alfvénic, but has effectively zero perpendicular field.

ties forbidden by the hydrodynamic jump conditions: in the evolution of an H II region, the fast-mode shock sent into the neutral gas by the fast-critical transition will act to generate these high transverse fields. In the obliquely-magnetized case, the fronts are significantly perturbed as long as the Alfvén speed in the neutral gas is greater than $c_1^2/2c_2$. However, the stability of parallel-magnetized weakly evolutionary IF means that the flow may still leave at the isothermal sound speed in the ionized gas over much of the surface of magnetized globules exposed to ionizing radiation fields.

Large ($\gtrsim 100\,\mu$G), highly ordered magnetic fields have been observed in the molecular gas surrounding some H II regions (e.g. Roberts et al. 1993; Roberts et al. 1995). Roberts et al. (1995) suggested that the highest observed magnetizations in S106 are associated with unshocked rather than shocked gas, as a result of the relatively low density and velocity shift observed for the strongly magnetized gas. They suggested that the magnetic field becomes tangled close to the IF, leading to the decrease in detectable magnetization.

It is interesting to compare these results with the example fast-critical front we discuss in Section 5. Scaling the parameters of this front to an exhaust hydrogen density of $10^4\,\mathrm{cm}^{-3}$, typical of an ultracompact H II region, a mean mass per hydrogen nucleus of 10^{-24} g, and a sound speed in the ionized gas of $10\,\mathrm{km\,s}^{-1}$, the limiting $1 \rightarrow 1$ front takes the flow from an upstream state with $n_\mathrm{H} = 5.03\times10^3\,\mathrm{cm}^{-3}$, $\boldsymbol{v} = (-0.0497, 0, 20.0)\,\mathrm{km\,s}^{-1}$ and $\boldsymbol{B} = (17.7, 0, 35.4)\,\mu$G to an exhaust with $n_\mathrm{H} = 10^4\,\mathrm{cm}^{-3}$, $\boldsymbol{v} = (0, 0, 10.1)\,\mathrm{km\,s}^{-1}$ and $\boldsymbol{B} = (35.4, 0, 35.4)\,\mu$G (while the fast-R-critical speed is almost exactly twice the exit speed of the front, this ratio decreases in more strongly magnetized fronts). The limiting $2 \rightarrow 2$ front takes the flow from $n_\mathrm{H} = 1.61\times10^5\,\mathrm{cm}^{-3}$, $\boldsymbol{v} = (1.78, 0, 0.625)\,\mathrm{km\,s}^{-1}$ and $\boldsymbol{B} = (671, 0, 35.4)\,\mu$G to the same final state. A fast-mode shock ahead of the front and at rest with respect to it would change the upstream state from that of the limiting $1 \rightarrow 1$ front to that of the limiting $2 \rightarrow 2$ front.

This fast-mode shock, which precedes a limiting fast-weak-D type front, boosts the x-component of the magnetic field from $18\,\mu$G to $670\,\mu$G, with a $20\,\mathrm{km\,s}^{-1}$ change in the z-velocity and only a $2\,\mathrm{km\,s}^{-1}$ change to the x-velocity component. A succeeding slow-mode shock would further increase the z-velocity component and gas density while weakening the x-component of magnetic field, without recourse to field-tangling. If we tentatively identify OH component B of Roberts et al. as fast-shocked material and component A as doubly-shocked material, component B is more edge-brightened and has a smaller blueshift than component A as would be expected. Component A is kinematically warmer and most blue shifted towards the centre of the region. The strong line-of-sight magnetic fields in S106 are seen at the edges of the region, in a 'toroidal' distribution. The (poorly resolved) line-of-sight velocity of component B has little gradient in the equatorial plane of the region, but this might result in part from a combination of flow divergence and the value of B_los (which is measured close to the centre of the region) being rather larger than that of B_z in our example. While the qualitative properties of this assignment are attractive, it remains to calculate a proper model tuned to the properties of the region, in particular its geometry. Nevertheless, the present discussion at least illustrates how both fast and slow shocks should be considered in the analysis of regions with well-ordered magnetization.

In future work, we will model in detail the global structure of magnetized H II regions and the local structure of photoevaporated magnetized clumps.

Acknowledgements.

We thank Sam Falle and Serguei Komissarov for helpful discussions on evolutionary conditions, and the referee for constructive comments which brought several issues into sharper focus. RJRW acknowledges support from PPARC for this work.

REFERENCES

Anderson J.E., 1963, Magnetohydrodynamic shock waves, MIT Press: Cambridge, Mass.

Axford W.I., 1961, Phil. Trans. A, 253, 301

Brio M., Wu C.C., 1988, J. Comp. Phys., 75, 400

Dyson J.E., 1994, in Ray T.P., Beckwith S.V., eds, Lecture Notes in Physics 431, Star Formation Techniques in Infrared and millimetre-wave Astronomy. Springer-Verlag, Berlin, p. 93

Dyson J.E., Williams D.A., 1997, The Physics of the Interstellar Medium (2nd edition), Institute of Physics Publishing: Bristol

Falle S.A.E.G., Komissarov S.S., 1997, in Computational Astrophysics, eds. Clarke D.A., West M.J., ASP Conf. Ser. 123, 66

Falle S.A.E.G., Komissarov S.S., Joarder P., 1998, MNRAS, 297, 265
Falle S.A.E.G., Komissarov S.S., 1999, J. Fluid Mech., submitted
Goldsworthy F.A., 1961, Phil. Trans. A 253, 277
Jeffrey A., Taniuti T., 1964, Non-linear Wave Propagation with Applications to Physics and Magnetohydrodynamics, Academic Press, London
Kahn F.D., 1954, Bull. Astr. Inst. Netherlands, 12, 187
Kennel C.F., Blandford R.D., Wu C.C., 1990, Phys. Fluids B, 2, 253
Lasker B.M., 1966, ApJ, 146, 471
Osterbrock D.E., 1989, Astrophysics of Gaseous Nebulae and Active Galactic Nuclei, University Science Books: California
Pilipp W., Hartquist T.W., 1994, MNRAS, 267, 801
Redman M.P., Williams R.J.R., Dyson J.E., Hartquist T.W., Fernandez B.R., 1998, A&A, 331, 1099 (Paper I)
Roberts D.A., Crutcher R.M., Troland T.H., Goss W.M., 1993, ApJ, 412, 675
Roberts D.A., Crutcher R.M., Troland T.H., 1995, ApJ, 442, 208
Spitzer L., 1978, Physical Processes in the Interstellar Medium, Wiley: New York
Wardle M., 1998, MNRAS, 298, 507
Williams R.J.R., Dyson J.E., 1996, MNRAS, 279, 987
Williams R.J.R., 1999, MNRAS, in press